PAPER

ELM-free and inter-ELM divertor heat flux broadening induced by edge harmonics oscillation in NSTX

IOP Publishing | International Atomic Energy Agency Nuclear Fusion

Nucl. Fusion **57** (2017) 126053 (8pp) https://doi.org/10.1088/1741-4326/aa8c4a

ELM-free and inter-ELM divertor heat flux broadening induced by edge harmonics oscillation in NSTX

K.F. Gan[1], J.-W. Ahn[2], T.K. Gray[2], S.J. Zweben[3], E.D. Fredrickson[3], F. Scotti[4], R. Maingi[3], J.-K. Park[3], G.P. Canal[5], V.A. Soukhanovskii[4], A.G. Mclean[4] and B.D. Wirth[1]

[1] University of Tennessee, Knoxville, TN, United States of America
[2] Oak Ridge National Laboratory, Oak Ridge, TN, United States of America
[3] Princeton Plasma Physics Laboratory, Princeton, NJ, United States of America
[4] Lawrence Livermore National Laboratory, Livermore, CA 94550, United States of America
[5] General Atomics, PO Box 85608, San Diego, CA 92186-5608, United States of America

E-mail: kgan@ppp.gov

Received 28 March 2017, revised 6 September 2017
Accepted for publication 13 September 2017
Published 26 October 2017

Abstract

A new $n = 1$ dominated edge harmonic oscillation (EHO) has been found in NSTX. The new EHO, rotating toroidally in the counter-current direction and the opposite direction of the neutral beam, was observed during certain inter-ELM and ELM-free periods of H-mode operation. This EHO is associated with a significant broadening of the integral heat flux width ($\lambda_{\rm int}$) by up to 150%, and a decrease in the divertor peak heat flux by >60%. An EHO induced filament was also observed by the gas puff imaging diagnostic. The toroidal rotating filaments could change the edge magnetic topology resulting in toroidal rotating strike point splitting and heat flux broadening. Experimental result of the counter current rotation of strike points splitting is consistent with the counter-current EHO.

Keywords: heat flux width, edge harmonic oscillation, strike points splitting, NSTX

(Some figures may appear in colour only in the online journal)

1. Introduction

A recent multi-machine study of the midplane scrape-off layer (SOL) power fall-off length, λ_q in current tokamaks indicates that for ITER, λ_q is expected to be very narrow, ~1 mm [1]. This result is consistent with the prediction from a heuristic drift-based theory [2]. However this theory does not consider the effects of edge magnetohydrodynamics (MHD). The narrow inter-ELM λ_q will result in a large peak heat flux, $q_{\rm peak}$ on the divertor in excess of the material limits of the plasma facing component (PFC). For ITER, the steady state heat flux limit is 10 MW m^{-2} [3]. However, edge MHD could be important in determining the divertor heat flux width. This paper describes experimental results that demonstrate that edge MHD activity, namely an edge harmonic oscillation (EHO) leads to a broadening of the divertor heat flux.

2. Background of EHO

An EHO is an edge localized, electromagnetic oscillation with multiple toroidal harmonics, which was first observed on DIII-D [4]. The EHO enhances the edge particle transport and is key to quiescent H-modes. It was found that the EHO can exist both for ELM-free phases and inter-ELM in standard type I ELM scenarios on DIII-D, and the EHO is not a saturated ELM precursor [5]. For the EHO in DIII-D, Infrared thermography (IRTV) shows a wide distribution of deposited heat flux in the divertor and on the baffle structure, in which the EHO was associated with an increase in divertor peak heat flux, especially for the inner target plate, and an extra peak in the heat flux profile existed away from the outer strike point. It is believed that the EHO produced a perturbation on trapped ion orbits resulting in beam ion orbit losses that may contribute

to the extra peak in the heat flux profile [6]. In DIII-D, EHO rotated in the direction of the neutral beam and was found to have no relationship with the plasma current direction [4].

The outer mode (OM) in JET may be related to the EHO [7]. By assuming a current filaments existed at $q = 4$ rational surface and comparison with Mirnov signal, a spontaneously formed closed current ribbon has been observed for the OM. It is located at the pedestal top, it is long-lived, and it regulates transport across the plasma pedestal, significantly delaying the appearance of ELMs. Periodic bursts of heat arrive away from the maximum deposition location, and this is consistent with the effect of a rotating current structure at the top of the pedestal: it can break toroidal symmetry and produce partial ergodisation of field lines increasing overall particle and heat flux across the pedestal. Additionally, a flux tube can escape through the broken separatrix (a homoclinic tangle) and lead to the toroidally localized heat pulses. However, the peak heat flux caused by OM in JET is very large, on the order of 30 MW m^{-2} [7]. When the current rotates toroidally, the footprint of strike point splitting on the divertor will rotate toroidally, and the heat flux at a given toroidal angle will show a radial propagation, which can be observed from figure 6 in [7]. The OM rotates toroidally along the co-current direction, and with the same direction as the main plasma toroidal rotation in JET [7].

EHO has also been previously found in NSTX when the ELMs were suppressed with lithium wall coating [8]. A number of diagnostics have confirmed $n = 4$–6 edge-localized and coherent oscillations in the 2–8 kHz frequency range. This EHO was observed to rotate with both the co-current and neutral beam direction, and it was not associated with any enhanced particle or heat transport in edge plasma.

This paper describes the observation of a different type of EHO, which rotates at counter-current direction and in the opposite direction from the neutral beam, which is different from in DIII-D, JET and the previous EHO observation in NSTX.

3. Broadening divertor heat flux width induced by EHO

For the divertor heat flux measurements in NSTX, a Santa Barbara focal plane (SBF161) infrared (IR) camera was used to measure the lower divertor temperature evolution with a spatial resolution of 6 mm/pixel and a frame rate of 6.3 kHz [9]. The heat flux is calculated by a 3D heat flux solver code, TACO [10]. In order to ensure a reliable heat flux calculation, TACO iterates on the heat transmission coefficient, α [11] until the total deposited energy on the divertor PFCs is constant after the end of discharge. The integral heat flux width is defined as $\lambda_{\rm int} = \left(\int \frac{q_{||}(s)\mathrm{d}s}{f_x(s)}\right) / \max(q_{||})$, where s is radial path length along the divertor, the $q_{||}(s)$ is the parallel heat flux on the middle which is calculated from the divertor heat flux at the location s, and $f_x(s)$ is magnetic flux expansion from the outboard midplane to the divertor location s. The deposited power to the divertor surface is obtained by integrating the heat flux in both the radial and toroidal directions: $P_{\rm div} = \int 2\pi R q(s)\mathrm{d}s$; this equation assumes toroidal symmetry. Figure 1 shows the EHO effect on the divertor heat flux.

A characteristic signature of the EHO is displayed in the MHD spectrogram: its harmonic structure, as shown in figure 1(*a*). Both the mode number and the mode rotation direction can be calculated from the Mirnov probs. In order to distinguish the modes direction, the negative and positive frequency is used to represent the different toroidal rotation direction. The negative frequency indicates that the mode rotates in the counter-current direction and in the opposite direction from the neutral beam. In NSTX, the neutral beam involves a co-current injection. The shot 132405 is a lower single null, ELM-free H mode with ~4 MW of injected neutral beam power with a plasma current, $I_{\rm p}$ ~600 kA, edge q_{95} ~ 10, $\beta_{\rm p}$ ~ 1.1, the core density as a fraction of Greenwald density $n_e/n_{\rm GW}$ ~ 0.49, and toroidal magnetic field, $B_{\rm T}$ ~ 0.45 T. The data shown in figure 1 is during the current flat-top. One can see clear harmonic oscillation with low frequency 2–4 kHz and low toroidal periodicity of $n = 1$–2 from panel (*a*). The fundamental frequency is ~2 kHz and its toroidal mode number is $n = 1$. The mode intensity in figure 1(*b*) shows the harmonic oscillation is $n = 1$ dominated. The gas-puffing imaging (GPI) diagnostic [13] uses a fast visible camera to record the 2D D_α (656 nm) line emission image near the separatrix at a resolution of 64 × 64 pixels with a frame rate of ~110 kHz, the pixel resolution is 3.8 mm × 3.8 mm, and the total viewable area is 24 cm × 24 cm. During shot 132405, the GPI diagnostic was operated passively, e.g. without active gas puffing. Figure 1(*c*) shows a spectrogram of D_α emission at the separatrix showing a ~2 kHz oscillation. This is consistent with an $n = 1$ mode, indicating that multiple harmonic oscillations exist in the edge plasma, so this harmonic oscillation could be considered as EHO. GPI does not observe the $n = 2$ mode oscillation as the magnetic signals. The reason could be that the $n = 2$ mode is too weak compared to the $n = 1$ mode, such that the intensity of the $n = 1$ mode is ~3 times stronger than the $n = 2$ mode.

Figure 1(*d*) shows the divertor heat flux evolution on the lower outer target plate. The red and orange dashed lines in figure 1 are marked for EHO appearance. We can see the $\lambda_{\rm int}$ ($q_{\rm peak}$) significantly increases (decreases) with the appearance of the EHO. Before the EHO, $\lambda_{\rm int}$ is ~0.016 m and $q_{\rm peak}$ is ~0.9 MW m^{-2}. When the EHO appears, $\lambda_{\rm int}$ increases to ~0.04 m and $q_{\rm peak}$ decreases to ~0.35 MW m^{-2}, as shown in figures 1(*e*) and (*f*). The decreasing in $q_{\rm peak}$ causes the increasing in $\lambda_{\rm int}$. This is due to the broadening of the divertor heat flux during EHO as shown in figure 1(*d*). When the EHO disappears at ~0.168 s (green dash line), the $\lambda_{\rm int}$ decreases and $q_{\rm peak}$ increases. The EHO is intermittent between 0.172 s and 0.178 s (orange dash line), as shown in figure 1(*a*) $n = 1$ mode. This intermittent EHO is not considered to be an ELM since there is no burst for the $P_{\rm div}$. The temporal evolution of $\lambda_{\rm int}$ and $q_{\rm peak}$ shows intermittent increasing and decreasing which is consistent with the intermittent nature of the EHO. However, the onset condition for this EHO is not yet understood. It is also clear that two $\lambda_{\rm int}$ peaks are observed just before 0.161 s (red dash line) in figure 1(*f*), consistent with the perturbation of Mirnov signal in figure 1(*b*). There is a

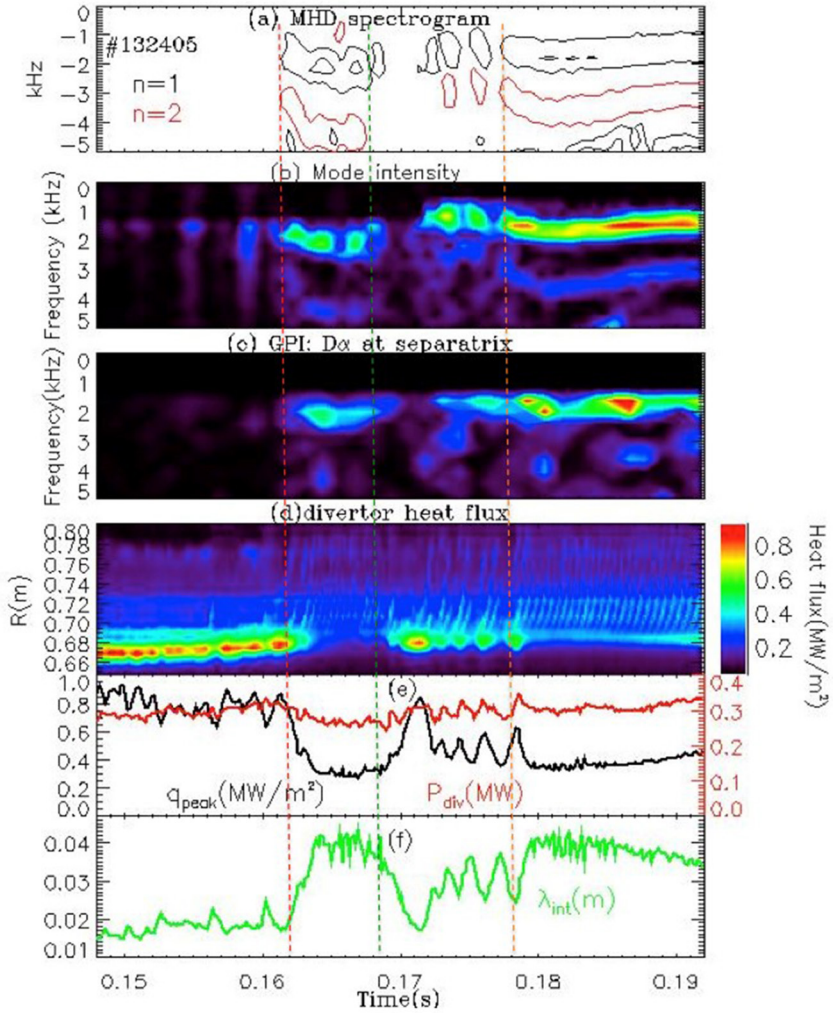

Figure 1. Broadening divertor heat flux measured during the EHO. Magnetic oscillation detected by Mirnov coil (*a*), relative mode intensity (*b*), D_α spectrogram at the separatrix measured by GPI diagnostic (*c*), the evolution of divertor heat flux on lower outer target plate (*d*), the divertor peak heat flux and deposited power on divertor (*e*) and integral heat flux width (*f*).

~2 kHz oscillation that exists on the divertor heat flux during this EHO, which is especially clear after 0.177 s, as shown in figure 1(*d*). Figure 2(*a*) shows the detail of the EHO induced heat flux oscillation, but with a much more refined time scale from 0.1826 s to 0.1863 s. The stripe in divertor heat flux moves radially in time; beginning to deposit heat onto the near strike point and then further out to the far strike point at a later time. The divertor heat flux is consistent with an EHO $n = 1$ mode in figure 2(*b*). The Mirnov signal were taken by data frequency filter (1.5–2.5 kHz) to get the magnetic signal from $n = 1$ mode.

The GPI field of view can be seen in figure 2(*d*). The black line is the separatrix as obtained from EFIT. Figure 2(*c*) shows the time evolution of D_α emission at separatrix. The oscillation of D_α at separatrix is consistent with the EHO $n = 1$ mode and the radial propagation heat flux. The 3 frames of GPI images in figure 2(*d*) were taken from the red dash line in figure 2(*c*). With the counter current EHO, a regular change can be observed from the GPI images: there is a fluctuation in GPI image, which moves in the positive z direction. The three frames at 183.858 ms, 183.867 ms and 183.883 ms show an EHO induced fluctuation that moves from the bottom image to the top image, the next fluctuation movements in the GPI image as the figure 2(*d*) will appear in next EHO $n = 1$ cycle.

In order to explain the movement shown in figure 2(*d*), along with the heat flux broadening, we define a hypothesis: a rotating filament is induced inside the separatrix by the EHO $n = 1$ mode. NSTX could not measure the poloidal number by the Mirnov probe, so the rational surface of the EHO could not be located. The plasma current is counter-clockwise direction in top view. There is evidence for the rotated filaments on plasma edge induced by EHO. If filaments exist at the $n = 1$ rational surface in figure 3, then when the EHO $n = 1$ mode rotates in counter current direction, the induced filament will also rotate in the counter current direction. This then would describe the observed movement of D_α emission propagating from the bottom to top as shown in figure 2(*d*). From the figure 2(*d*), it indicates that the EHO location could be really close to the separatrix. However, the mode could not be located without poloidal mode number. The distance between the $q = 8$ (15) rational surface and middle-plane separatrix is ~18 (3) mm, which is really close to the separatrix. Assume the EHO $n = 1$ mode existed between $q = 8$ and $q = 15$ rational surface. From the figure 3, the toroidal angle which

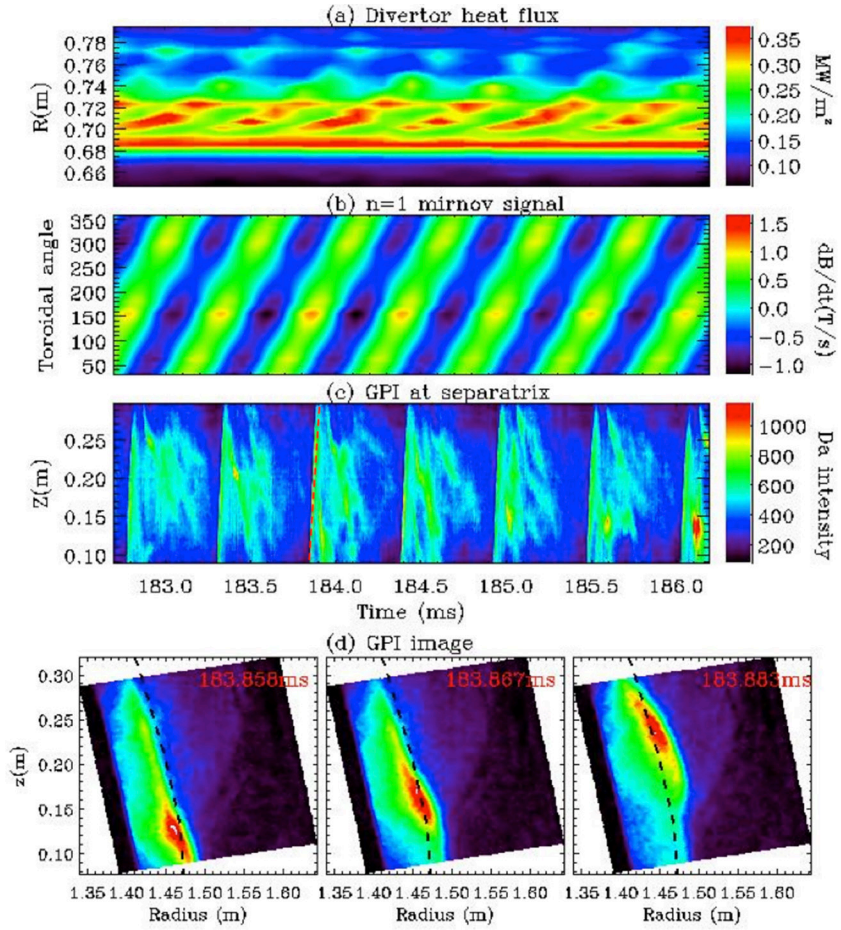

Figure 2. NSTX shot 132405: heat flux evolution on lower outer divertor target plate (*a*), Mirnov signal of $n = 1$ (*b*), temporal evolution of GPI data at separatrix (*c*) and 3 frames of GPI images, black line indicates the separatrix.

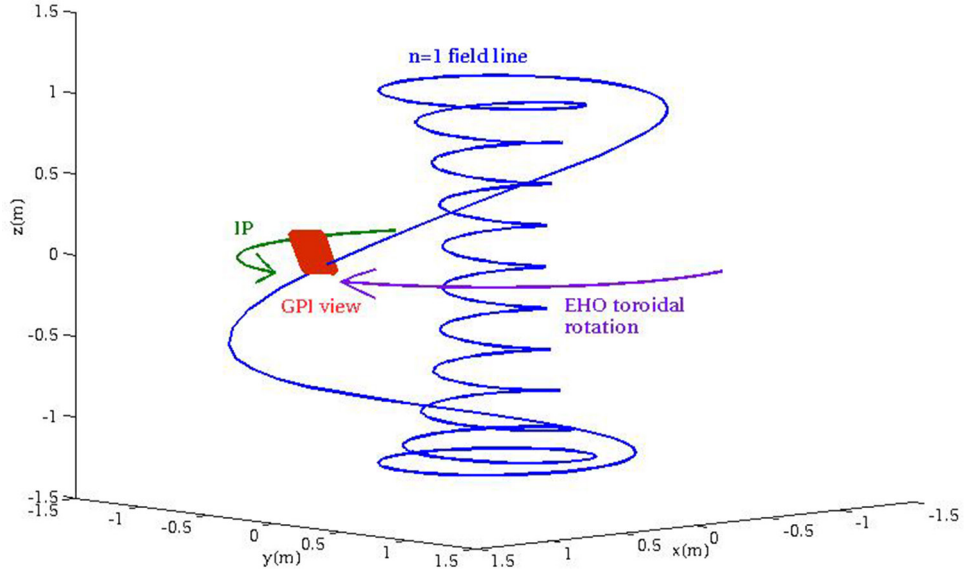

Figure 3. $n = 1$ field line and GPI field of view.

the $n = 1$ field line should rotate to pass the GPI field of view can be calculated. Meanwhile, from the GPI movie as the figure 2(*d*), the time which the $n = 1$ field line should rotate to pass the GPI field of view can be estimated. Then the toroidal rotation velocity of the EHO $n = 1$ mode can be calculated. The calculated toroidal rotation velocity is 1.04–1.18 $\times$ 10^4 rad s^{-1} from the $q = 8$ to $q = 15$, similar as the measured value (1.13 $\times$ 10^4 rad s^{-1}) by the Mirnov probes. It indicated that the GPI observation in figure 2(*d*) is induced by toroidal rotation of EHO $n = 1$ field line. The EHO induced filament

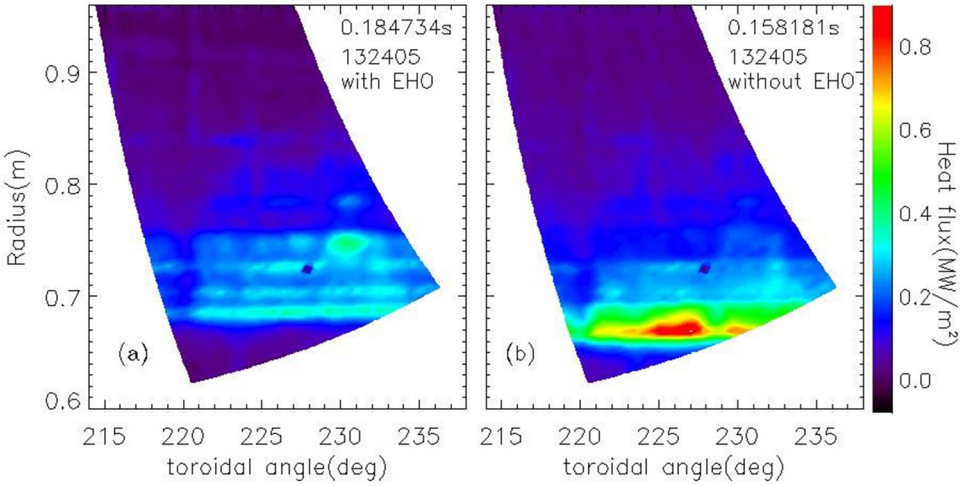

Figure 4. Strike point splitting induced by EHO, 2D heat flux distribution with EHO (*a*) and without EHO (*b*).

could be considered as a current filament, since the Mirnov probe measured the magnetic fluctuation signal in figure 2(*b*). A current filament appears on the edge plasma: it may break toroidal symmetry and induce strike point splitting.

Figure 4 shows a 2D divertor heat flux (*a*) during an EHO and (*b*) with no EHO for the shot 132405. While no strike point splitting is observed in the heat flux profile when the EHO is not present (figure 4(*b*)), one can see several peaks in the heat flux distribution in figure 4(*a*), which is a clear indication of strike point splitting. Because of these multiple peaks, the Eich fitting method [12] could not be used to calculate λ_q. It is conjectured that the multiple heat flux peaks are induced by the EHO since the strike point splitting disappears without the EHO. The footprint of the strike point splitting on the divertor is non-axisymetric, the stripes location change with toroidal angle [14], which is hard to see in figure 4 beacuase of the narrow field of IR view. It is suspected that the strike point spliting will change in time due to the toroidal rotation of the $n = 1$ mode. In figure 2(*b*), one can see the EHO $n = 1$ mode rotate from smaller to larger toroidal angle. Thus the observed strike point splitting of the heat flux footprint should also rotate in the same direction as the $n = 1$ mode, and then the heat flux stripes at a given toroidal angle will propagate radially as shown in figure 2(*a*).

The EHO usually exists first at ELM-free periods after L–H transition, when the ELM-free transits to ELMy H mode, the counter current EHO still exists during inter-ELM periods. A clear, low frequency oscillation of between 2–10 kHz with low toroidal periodicity of $n = 1$–4 can be seen in figure 5(*a*), which appears during inter-ELM. The shot 132405 is a lower single null H mode with ~4 MW of injected neutral beam power, a plasma current, I_p ~ 700 kA, edge q_{95} ~ 9, n_e/n_{GW} ~ 0.59 and β_p ~ 0.9. In this shot, the EHO is still an $n = 1$ dominated EHO, and the heat flux oscillation is 2 kHz as the EHO $n = 1$ mode. A heat flux profile with EHO is shown with red line in figure 5(*c*), this heat flux profile is averaged by several inter-ELM periods from the figure 5(*b*). An averaged inter-ELM heat flux profile without EHO is also shown with black line in figure 5(*c*), which the plasma current, injected neutral beam power and f_x at the strike points are the same as

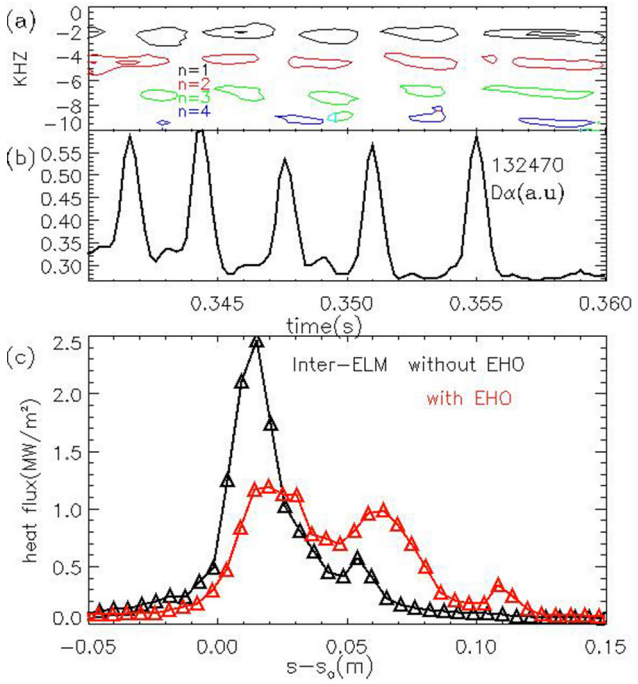

Figure 5. Observation of the EHO during inter-ELM. (*a*) MHD spectrogram, (*b*) divertor Da signal and (*c*) compariron of heat flux profile at inter-ELM with EHO (red line) and without EHO (black line), where the s–s_o is the distance from the strike point.

the red line in figure 5(*c*). q_{peak} is ~2.5 MW m^{-2} during the inter-ELM period without an EHO. While, a reduced q_{peak} of ~1 MW m^{-2} is observed with the EHO. The inter-ELM heat flux profile is much wider with EHO than without EHO, the λ_{int} is 0.023 m with EHO from figure 5(*c*); while λ_{int} is ~0.01 m without EHO as shown in figure 5(*c*). This data indicates the EHO can broaden the inter-ELM divertor heat flux and decrease the q_{peak}. The EHO disappears when the ELM happens, as show in figure 5. It is hard to consider the counter-current EHO as an ELM precursor, since the counter-current can be a long live mode. Figure 6(*b*) shows the Mirnov signal of EHO $n = 1$ mode. An ELM apears at 352.7 ms, which can be seen from divertor lithium emission in figure 6(*a*). The EHO $n = 1$ mode in figure 6(*a*) and stripe movement in

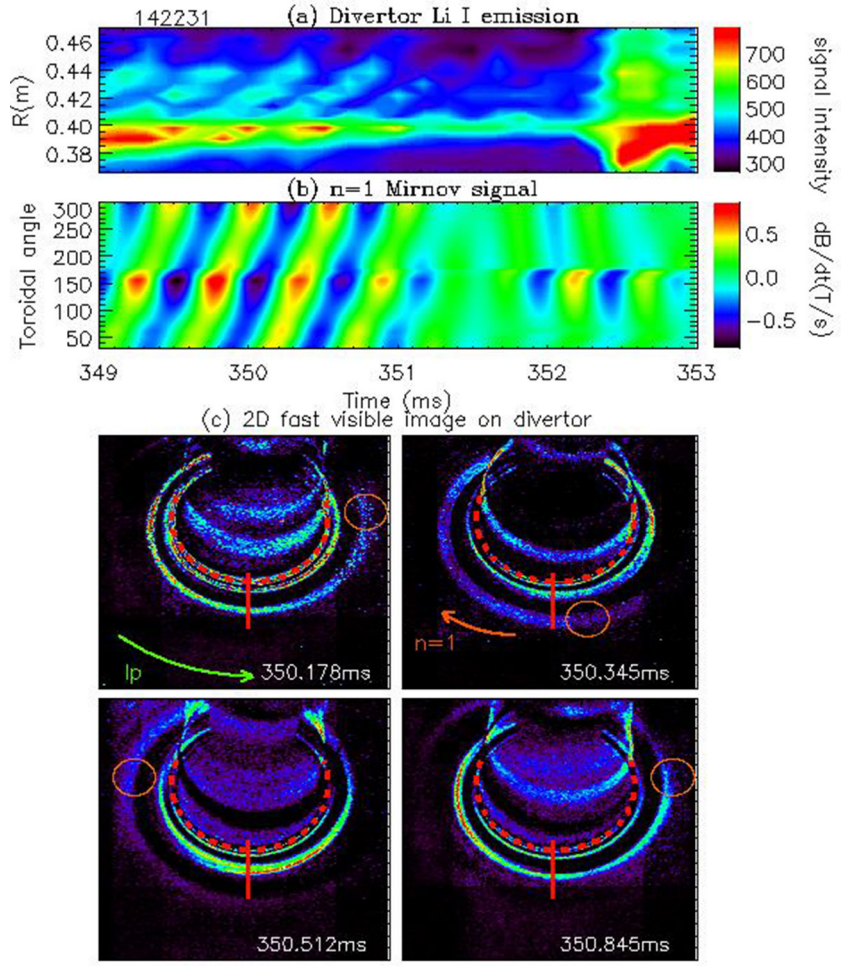

Figure 6. Observation of the counter-current rotation for the strike points splitting induced by EHO $n = 1$ mode. (*a*) The evolution of the divertor Li I emission at one toroidal location, (*b*) Mirnov signal of the EHO $n = 1$ mode, (*c*) 2D fast visible image in lower divertor, red dash line indicates the outer strike points.

figure 6(*a*) can disppear before ELM happen. It indicates the EHO is not a saturated ELM precursor.

4. The evidence for toroidal rotation of strike points splitting induced by $n = 1$ mode

It is hard to observe the toroidal rotation of strike points splitting by the IR camera in NSTX since the small IR image of <5% of the toroidal extent of the divertor, as shown in figure 4. A fast visible camera was applied to get wide range image of over 50% of the toroidal extent of the divertor in NSTX [15], which can measure large scale of the strike point splitting. The fast visible camera observed the Li I emission (670.8 nm) with 256 × 208 pixels given a spatial resolution of 0.8 cm and up to 100 kHz frame rate. Figure 6(*a*) shows the low divertor Li I image with an EHO $n = 1$ mode and the divertor Li I image is 6 kHz data. The shot 142231 is a lower single null with ~1 MW of injected neutral beam power, I_p ~ 800 kA and f_x ~ 14 at the outer strike points. The large f_x make it is easy to identify the structure of strike point splitting by the visible camera. The EHO $n = 1$ mode is shown in figure 6(*b*). The divertor Li emission at one toroidal location (red solid line in figure 6(*c*)) move outward with 2 kHz in figure 6(*a*), which is consistent with the $n = 1$ mode in figure 6(*b*). This phenomenon is the same as the figure 2(*a*). Unfortunately, there is no IR data for the shot 142231. An ELM appears at 352.7 ms, which can be seen from divertor lithium emission in figure 6(*a*). The stripe movement and EHO $n = 1$ mode can disappear before ELM happen, as shown in figure 6(*b*). It indicates the EHO is not an ELM precursor.

In order to show the rotation of the strike point splitting, four frames at 350.178, 350.345 ms, 350.512 ms and 350.845 ms show the 2D lower divertor visible image in figure 6(*c*). The red and brown arrow indicate the direction of plasma current and $n = 1$ rotation respectively. The red dash line in figure 6(*c*) indicates the outer strike point. There is just one helical stripe in figure 6(*c*) indicates it could be $n = 1$ strike point splitting. It is clear to see the distance between the helical stripe and outer strike points increases at co-current direction, which is very good agreement with homoclinic tangle by an $n = 1$ (as shown in figure 3). The yellow circle in figure 6(*c*) shows the tail of the helical stripe. From the tail of helical stripe, it is clear to see the footprint of strike points splitting rotates at counter current direction from 350.178 ms to 350.845 ms. The distance between the helical stripe and the strike points splitting decreases as the counter

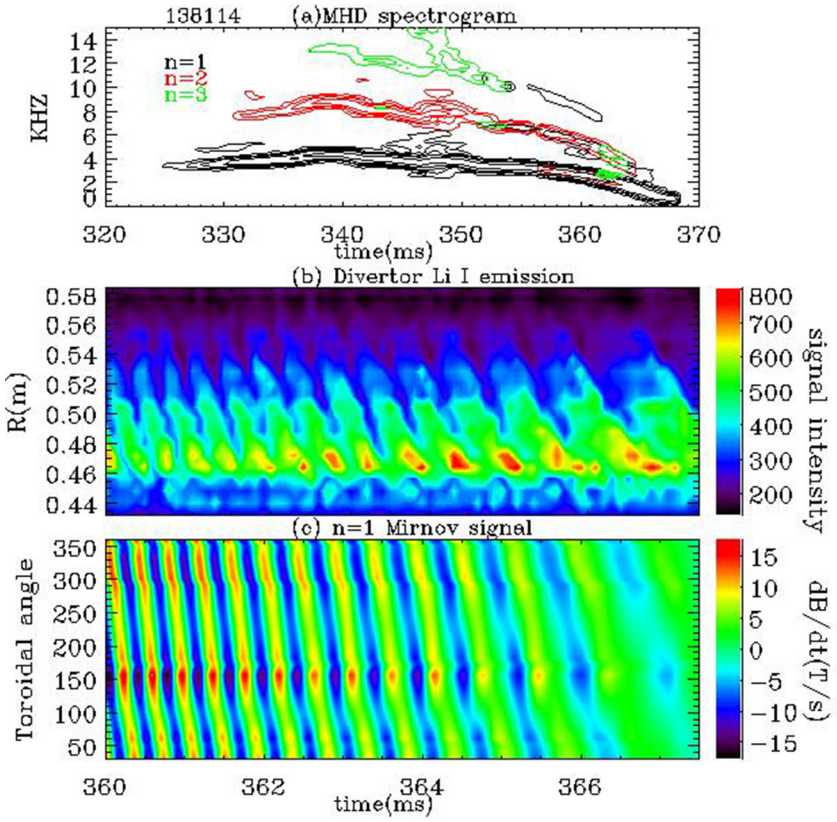

Figure 7. Observation of the stripe movements due to the co-current $n = 1$ mode. (*a*) MHD spectrogram, (*b*) The evolution of the divertor Li I emission at one toroidal location and (*c*) Mirnov signal of the EHO $n = 1$ mode.

current direction. When the footprint of strike points splitting rotates at counter current direction, the distance between this helical stripe and the strike point at a given toroidal location will increase, which can be used to explain the phenomenon in figure 6(*a*). The toroidal rotation of the strike points splitting in figure 6(*c*) have the same rotation velocity and rotation direction as the counter-current $n = 1$ mode, which indicate the strike points splitting is induced by the $n = 1$ mode. This is also first time to directly describe a MHD induced strike point splitting rotate toroidally. The heat flux at a given toroidal location changed due to a slow tearing mode was also found in DIII-D [16, 17]. The 2D strike points splitting due to a co-current EHO with $n = 3$–8 was also observed in NSTX [18].

For the co-current MHD induced strike point splitting in NSTX, it could be predicted that the stripes at one toroidal location will move to the strike points. To be comparison, the divertor stripe movement due to a co-current MHD is shown in figure 7. The 138114 is H mode, with 2.5 MW of neutral beam and $I_p \sim 900$ kA. The MHD spectrogram shown in figure 7(*a*) is probably a kink mode. From the $n = 1$ Mirnov signal in figure 7(*b*), one can see the rotation direction of $n = 1$ mode is different compare to the EHO $n = 1$ mode in figure 2(*b*). The figure 7(*b*) shows the divertor Li emission at one toroidal location, which the divertor Li emission is 10 kHz data. From 360 to 367 ms, the frequency of $n = 1$ mode gradually decreases from 3 kHz to 1 kHz. We can see the oscillation of the divertor lithium emission is consistent with the co-current $n = 1$ mode, one cycle of $n = 1$ rotation induces one stripe movement. The stripe in figure 7(*b*) move inside to the outer strike points, which is difference from figures 2(*a*) and 6(*a*). It could be explained by the different rotation direction of $n = 1$ mode. The footprint of strike points as in figure 6(*c*), when the $n = 1$ mode induced strike point splitting rotate as co-current direction, that will make the stripe in divertor at one toroidal location move to the outer strike points. When frequency of $n = 1$ mode decreases, the strike points splitting rotate slower, then the stripe movement become slower, as shown in figure 7(*b*). It indicates the toroidal rotation of strike point splitting is induced by the co-current $n = 1$ mode.

5. Summary and discussion

A new $n = 1$ dominated EHO rotating toroidally in the counter-current (and counter neutral beam) direction was observed during certain inter-ELM and ELM-free periods of H-mode operation in NSTX. Although both current theory [2], and experimental results [1] predict a very small λ_{int} for ITER. The λ_q scaling data in figure 3 from [1] really scatter for NSTX data, λ_q from part of points are much larger than the scaling value. The counter current EHO is observed to lead to a significant broadening in integral heat flux width (λ_{int}) by up to 150%, and a decrease in divertor peak heat flux by >60%. Multiple peaks appear in the heat flux profile in the presence of an EHO. This is believed to be due to an EHO-induced filament rotating around the separatrix in the counter-current direction. The toroidally rotating filaments could change

the edge magnetic topology and broaden the heat flux profile via strike point splitting, which was clearly observed in the divertor heat flux footprint. Because of the EHO toroidal rotation, the strike point splitting will also rotate toroidally. Experimental observation of stripe movements in heat flux profile and 2D strike points splitting rotation show consistent trend with the toroidal rotation of EHO $n = 1$ mode. When a $n = 1$ mode rotates as co-current direction, that will make the difference direction of stripes movement.

The mechanism for the counter current EHO appearance is not yet understood in NSTX. The EHO is located near the separatrix. It might easily affect the edge magnetic topology and spread the heat flux distribution by strike point splitting. Although the intensity of co-current EHO and counter-current EHO is comparable, the NSTX co-current EHO existed at pedestal [8], while the counter-current EHO is really close to the separatrix. It is more difficult affect the separatrix for the co-current EHO then the counter-current EHO. That could explain the NSTX co-current EHO do not affect the particle transport to the divertor. The increased divertor heat flux width and decreased q_{peak} has also been observed by applying external magnetic perturbations in DIII-D [16]. Large λ_{int} was also observed during inter-ELM with a ~5 khz $n = 2$ single mode in NSTX [19]. It is thus suspected that edge MHD, not only EHO, could affect the divertor heat flux distribution. In particular, if the counter current EHO in NSTX, or other edge MHD, occur in future fusion tokamaks, this could reduce the PFC heat load through divertor heat flux spreading and q_{peak} reducing. However, the counter-current EHO require further research to fully identify the underlying mechanism.

Acknowledgment

This work was supported by the US DOE contract DE-AC05-00OR22725 (ORNL) and DE-SC0008309 (UTK).

References

[1] Eich T. *et al* 2013 *Nucl. Fusion* **53** 093031
[2] Goldston R.J. 2012 *Nucl. Fusion* **52** 013009
[3] Pitts R.A. 2009 *Phys. Scr.* **T138** 014001
[4] Burrell K.H. 2009 *Nucl. Fusion* **49** 085024
[5] Burrell K.H. 2003 *U.S.-EU Transport Task Force Meeting, Madison, USA* (https://fusion.gat.com/pubs-ext/MISCONF03/Burrell_pres.pdf)
[6] Lasnier C.J. 2003 *J. Nucl. Mater.* **313–6** 904–8
[7] Solano E.R. 2010 *Phys. Rev. Lett.* **104** 185003
[8] Park J.-K. 2014 *Nucl. Fusion* **54** 043013
[9] Ahn J.-W. *et al* 2010 *Rev. Sci. Instrum.* **81** 023501
[10] Gan K.F. *et al* 2013 *Rev. Sci. Instrum.* **84** 023505
[11] Herrmann A. *et al* 2001 *Proc. 28th EPS Conf. on Controlled Fusion and Plasma Physics (Madeira, Portugal, 2001)* (www.cfn.ist.utl.pt/EPS2001/CD/pdfs/P5.104.pdf)
[12] Eich T. *et al* 2011 *Phys. Rev. Lett.* **107** 215001
[13] Zweben S.J. *et al* 2010 *Phys. Plasmas* **17** 102502
[14] Ahn J.-W. *et al* 2014 *Plasma Phys. Control. Fusion* **56** 015005
[15] Scotti F. *et al* 2012 *Rev. Sci. Instrum.* **83** 10E532
[16] Evans T.E. 2005 *J. Phys., Conf. Ser.* **7** 174–90
[17] Ciro D. *et al* 2017 *Nucl. Fusion* **57** 016017
[18] Scotti F. 2017 *Nucl. Mater. Energy* **000** 1–6
[19] Gan K. *et al* 2015 *18th Int. Spherical Torus Workshop, Princeton, USA* (https://nstx.pppl.gov/DragNDrop/Scientific_Conferences/ST_Workshop/STW15-Princeton/presentations/Posters/Gan_poster_ISTW2015.pdf)